Am J Physiol Gastrointest Liver Physiol 322: G446–G456, 2022.
First published February 9, 2022; doi:10.1152/ajpgi.00238.2021

american physiological society

AMERICAN JOURNAL OF PHYSIOLOGY
GASTROINTESTINAL AND LIVER PHYSIOLOGY

RESEARCH ARTICLE

Angiotensin receptor blocker alleviates liver fibrosis by altering the mechanotransduction properties of hepatic stellate cells

Zisheng Huang,[1,2] Mahmoud Osman Khalifa,[1,2] Peilin Li,[3] Yu Huang,[3] Weili Gu,[3] and Tao-Sheng Li[1,2]

[1]*Department of Stem Cell Biology, Atomic Bomb Disease Institute, Nagasaki University, Nagasaki, Japan;* [2]*Department of Stem Cell Biology, Nagasaki University Graduate School of Biomedical Sciences, Nagasaki, Japan; and* [3]*Department of Hepatopancreatobiliary Surgery, Guangzhou First People's Hospital, Guangzhou, Guangdong, China*

Abstract

Angiotensin receptor blockers have been reported to be beneficial to liver fibrosis, but the relevant molecular and cellular mechanisms remain unclear. We herein investigated whether low-dose angiotensin receptor blocker alleviated liver fibrosis through mechanotransduction regulation. Hydrostatic pressure-induced liver fibrosis model was established in mice by ligating partially the inferior vena cava, and then randomly received a very low dose of losartan (0.5 mg/kg) or placebo treatment for 8 weeks. We found that losartan administration interfered the expression of several mechanotransductive molecules, and effectively alleviated liver fibrosis. Using a commercial device, we further confirmed that ex vivo loading of hepatic stellate cells to 50 mmHg hydrostatic pressure for 24 h significantly upregulated RhoA, ROCK, AT1R, and p-MLC2, which was effectively attenuated by adding 10 nM losartan in medium. Our in vivo and ex vivo experimental data suggest that low-dose angiotensin receptor blockers may alleviate hydrostatic pressure-induced liver fibrosis by altering the mechanotransduction properties of hepatic stellate cells.

NEW & NOTEWORTHY Our ex vivo and in vivo experiments clearly indicated that low-dose losartan alleviated liver fibrosis, likely by modulating the mechanotransduction properties of HSCs. Uncovering the biomechanical signaling pathway of ARB treatment on liver fibrosis will be helpful to develop novel molecular targeting therapy for liver diseases.

angiotensin receptor blocker; hepatic stellate cells; hydrostatic pressure; liver fibrosis; mechanotransduction

INTRODUCTION

Fibrosis generally occurs in liver with chronic injury or inflammation (1). The key cellular mediator of liver fibrosis is well known as the hepatic stellate cells (HSCs), which serves as the primary collagen-producing cells when activated (2). Therefore, reducing the activity of HSCs is considered a viable approach for the prevention and treatment of liver fibrosis (3).

Cells in our body are always perceiving the dynamic changes of various surrounding biomechanics, such as the hydrostatic pressure generated by interstitial fluid and the stiffness generated by extracellular matrix (ECM) accumulation (4). The molecular process in which cells convert physical cues into biological responses when subjected to mechanical stimuli is collectively referred to mechanotransduction, which is of fundamental importance to modify the biological properties of cells (5).

In the diseased liver, the intrahepatic hydrostatic pressure is commonly elevated due to the increased production of inflammatory cytokines and enhanced vascular permeability (6). As the biological characteristics of HSCs can be largely affected by biomechanics in surrounding tissue microenvironment (7), the elevation of hydrostatic pressure in diseased liver may modify the mechanotransduction properties of HSCs to regulate the development and progression of liver fibrosis. Therefore, the interference of mechanotransduction signaling to HSCs is considered an effective therapeutic strategy on liver fibrosis (8).

Mechanical stresses have been demonstrated to upregulate the angiotensin II type 1 receptor (AT1R) in cardiomyocytes and vascular smooth muscle cells (9–11), indicating the potential role of AT1R in mechanotransduction. It has been shown that the blockade of AT1R by angiotensin receptor blocker (ARB), such as losartan, protects against cardiac fibrosis by modulating mechanotransduction pathways, including Ras homolog family member A (RhoA) and its downstream effectors of Rho-associated protein kinase (ROCK) and myosin light chain (MLC) (12, 13). In addition, losartan has been demonstrated to effectively relieve acute lung injury caused by mechanical stimulation and mitigate liver fibrosis caused by nonalcoholic steatohepatitis in rat (14, 15). However, it is asked to further confirm the probable benefit and the relevant mechanism of ARB on liver fibrosis. Therefore, this study was proposed to examine the hypothesis that ARB may alleviate liver fibrosis by altering the mechanotransduction properties of HSCs.

Correspondence: W. Gu (lili-6423@163.com); T.-S. Li (litaoshe@nagasaki-u.ac.jp).
Submitted 21 July 2021 / Revised 11 January 2022 / Accepted 2 February 2022

For in vivo experiment, losartan was given to mice after partial ligation of inferior vena cava (IVC). We observed that losartan administration at a low dose significantly alleviated liver fibrosis and interfered several molecules related to mechanotransduction pathway. We also ex vivo loaded primary human HSCs to 50 mmHg hydrostatic pressure and found that losartan effectively mitigated the hydrostatic pressure-induced alternations of AT1R expression and mechanotransduction properties in HSCs.

MATERIALS AND METHODS

Animals

Adult C57BL/6 mice (10 wk, CLEA, Japan) were maintained in a temperature- and light-controlled facility and permitted ad libitum consumption of water and standard pellet chow. All animal experiments were approved by the Institutional Animal Care and Use Committee of Nagasaki University (No. 1608251335-9) and carried out in accordance with institutional guidelines.

Partial IVC Ligation Model and Losartan Treatment

Partial IVC ligation was performed as described previously (16). Briefly, the abdomen of mouse was opened below the xiphoid process after the induction of general anesthesia. The suprahepatic IVC was exposed after the falciform ligament was divided (Fig. 1*A*). We separated the IVC and placed a small tube (0.9 mm diameter) along with the anterior surface of IVC (Fig. 1*B*). The tube was immediately and gently removed after tightly ligating together with the IVC (Fig. 1, *C* and *D*). The abdomen was then closed with a running suture of the peritoneal muscle/fascia followed by closure of the skin. Removing the 0.9-mm diameter tube from ligation was expected to reduce the cross-sectional area of IVC by ~80% based on previous report (16).

After all procedures were completed, mice were randomly given with losartan (WAKO) at a final concentration of 2.3 mg/L, which provided an estimated daily dose of 0.5 mg/kg (Losartan group, n = 6 mice) or without addition of any drug (IVCL group, n = 6 mice) in their drinking water. Treatments were continued until the cessation of experiments. As a control, mice were received a sham operation including all above steps with the exception of partial IVC ligation (Sham group, n = 6 mice).

Tissue Sampling and Serum Analyses

The mice were euthanized 8 wk postoperatively. Before euthanasia of each mouse, whole blood was collected from IVC and serum was separated. The levels of serum alanine aminotransferase (ALT) and aspartate aminotransferase (AST) were sent out for measuring by Nagahama Life Science Laboratory.

The suprahepatic IVC was then transected, and the liver was perfused with PBS through the portal vein to remove circulating blood and fibrinogen. The spleen and liver were harvested and weighed, and the spleen-to-body and liver-to-body weight ratios were calculated. Liver tissues were fixed in 4% paraformaldehyde and embedded into paraffin block. Tissue sections of ~5-μm thickness were used for histological analysis.

Masson's Trichrome Staining

Liver tissue sections were deparaffinized and rehydrated. Masson's trichrome staining was performed using Trichrome Stain (Masson) Kit (Sigma Aldrich), as described by the manufacturer, and then observed under an optical microscope (Olympus IX71, Olympus).

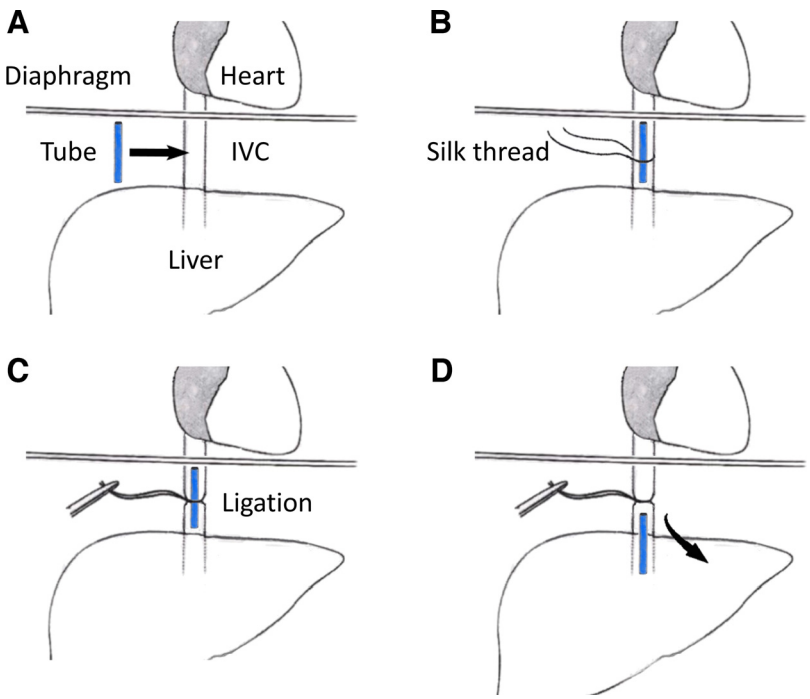

Figure 1. Schematic illustration of partial inferior vena cava ligation experimental model. *A*: the suprahepatic inferior vena cava (IVC) was isolated. *B*: a tube of 0.9 mm diameter was placed on the anterior surface of the IVC and a 7.0-silk thread was used to coil the IVC and the tube. *C*: the IVC and tube were then tightly tied around. *D*: the tube was then removed out.

Immunohistochemistry

Immunohistochemistry analysis on the liver tissues was performed to understand the relevant mechanism. Briefly, liver tissue sections were blocked with 10% bovine serum albumin and then incubated with primary antibodies (Supplemental Table S1; see https://doi.org/10.6084/m9.figshare.18133628) overnight at 4°C, followed by incubation with secondary antibodies (Supplemental Table S2) for 1 h at room temperature in the dark. Sections were then mounted with medium containing DAPI.

Apoptotic cells were detected by the usage of TUNEL staining kit (Abcam, Cat. No. ab66108) according to the manufacturer's instructions. Briefly, sections were incubated with DNA labeling solution for 60 min at 37°C, followed by the addition of PI/RNase A solution for 30 min.

Immunofluorescences of stained liver tissues were detected using an inverted fluorescence microscope (Olympus FV10i, Olympus). For each staining, at least 10 images were taken from randomly selected fields at ×60 magnification, and the mean fluorescence intensity was measured by ImageJ software.

Human HSCs

Primary human HSCs were purchased from ScienCell Research Laboratories (ScienCell). Cells were expanded by using stellate cell medium (ScienCell), in a humidified incubator under 5% CO_2 and 95% air at 37°C. The third passaged cells were used for the following experiments.

Ex Vivo Hydrostatic Pressure Loading of Human HSCs

A pneumatic pressurizing system (Strex, Inc.) was used to induce hydrostatic pressure. Briefly, HSCs were seeded in 60-mm diameter culture dishes (5×10^4 cells/dish) and four-well culture chamber slides (2×10^4 cells/well). Cells were incubated for 3 days to form ~70% confluent, and then half of the culture dishes and slides were randomly selected to be loaded by 50 mmHg hydrostatic pressure for

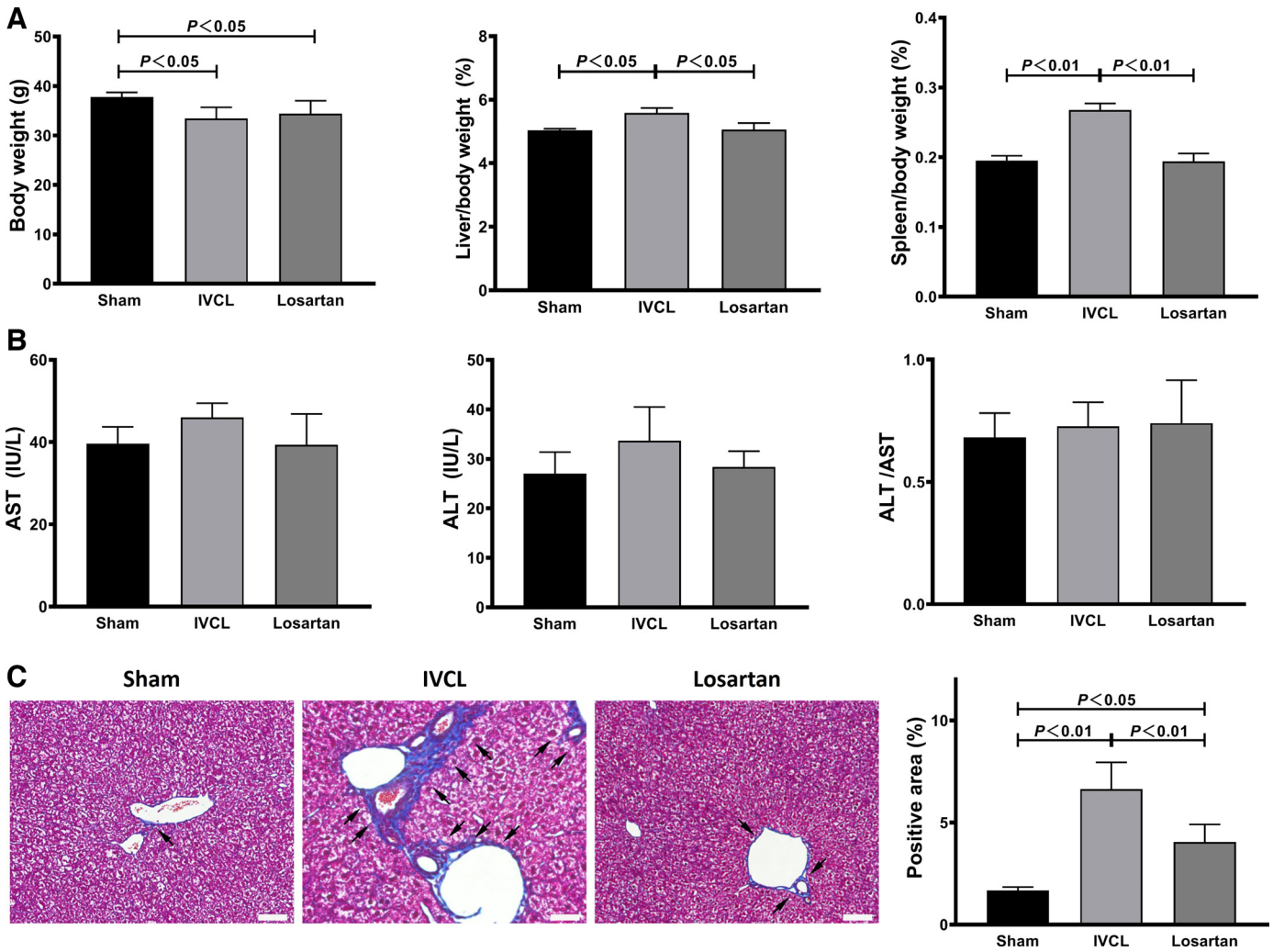

Figure 2. Systemic and local findings in liver of mice after treatment. *A*: body weight of mice are shown, and spleen-to-body weight ratio and liver-to-body weight ratios are calculated. *B*: the levels of ALT and AST, in serum of mice are shown, and the ALT/AST ratio is calculated. *C*: representative images of Masson's trichrome staining are shown, and black arrows indicate the fibrotic region of positive staining. Semiquantitative data on fibrotic area in liver are presented. Scale bars = 500 μm. ALT, alanine aminotransferase; AST, aspartate aminotransferase.

24 h, with or without the addition of 10 nM losartan in medium. We used 50 mmHg for experiments based on previous reports (17, 18), as well as the information from our preliminary experiments.

Reverse Transcription-Quantitative Polymerase Chain Reaction

Reverse transcription-quantitative polymerase chain reaction (RT-qPCR) was performed to evaluate the expression of *AT1R*, *RHOA*, *ROCK1*, *ROCK2*, *ACTA2*, *TGFB1*, and *COL1A1*. Briefly, total RNA was isolated from the HSCs using QuickRNA MicoroPrep Kit, and 1.25 μg RNA was reverse-transcribed using SuperScript VILO cDNA Synthesis Kit (Thermo Fisher Scientific). Quantitative PCR was carried out with SYBR Green real-time PCR Master Mix (Toyobo). The reactions were performed on a CFX96 real-time PCR System (Bio-Rad). The primer sequences were shown as supplementary information (Supplemental Table S3). *GAPDH* was used for normalization.

Immunocytochemistry

HSCs were fixed by 4% paraformaldehyde and then blocked by 10% bovine serum albumin. After overnight incubation with primary antibodies (Supplemental Table S1), cells were incubated with secondary antibodies (Supplemental Table S2) for 1 h at room temperature and then mounted with medium containing DAPI. F-actin fibers were stained with TRITC-phalloidin in mounting medium (Vector Labs). Immunofluorescences of stained cells were detected using an inverted fluorescence microscope (Olympus FV10i, Olympus). For each staining, 10 images were taken from randomly selected fields at ×60 magnification, and the mean fluorescence intensity was measured by ImageJ software.

Statistical Analysis

All the results were presented as means ± SD. Statistical significance was determined by one-way analysis of variance (ANOVA) followed by Turkey's test (GraphPad

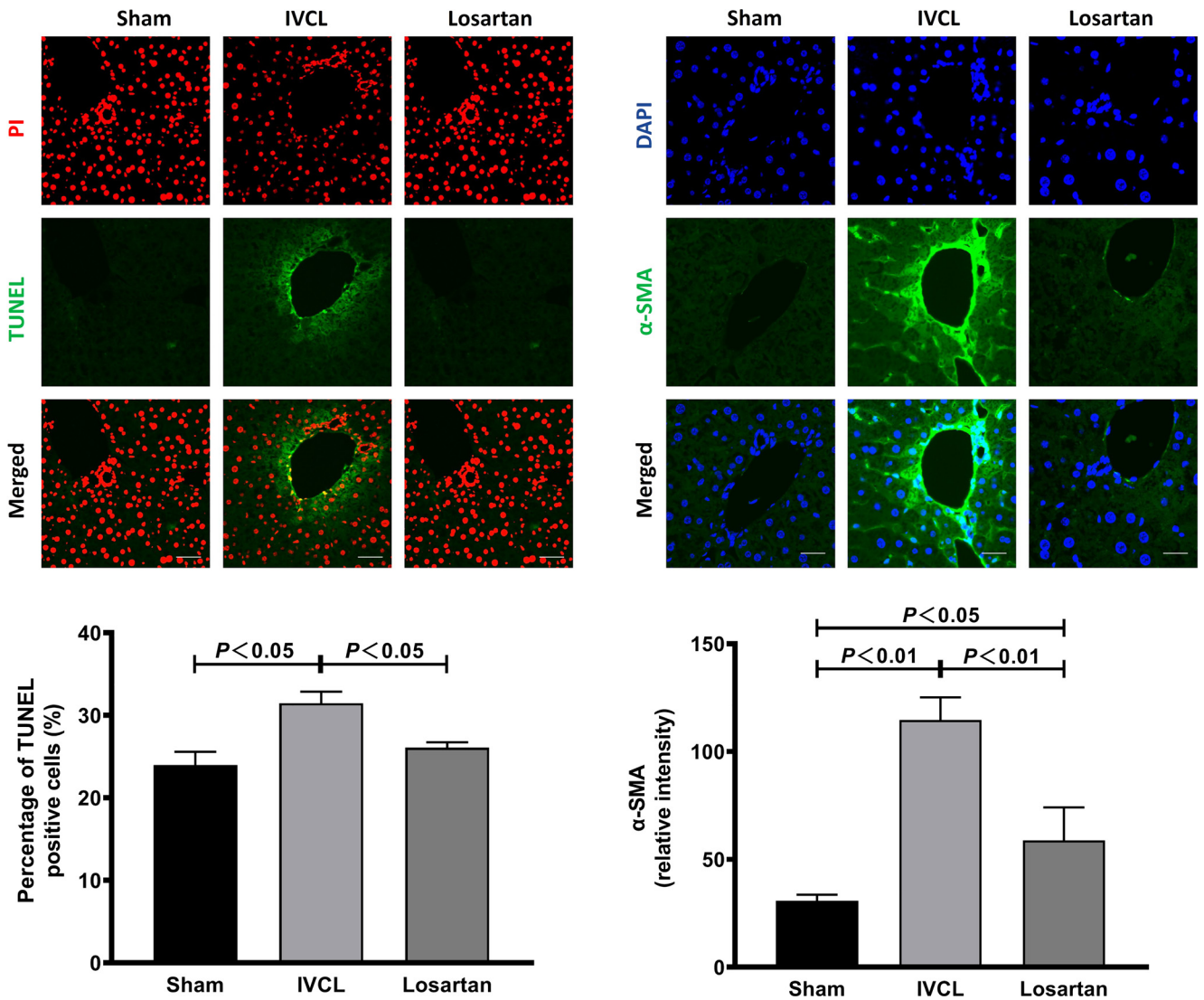

Figure 3. Apoptotic cells and the expression of α-SMA in liver of mice after treatment. Representative images (*top*) and semiquantitative data (*bottom*) on the TUNEL staining and immunofluorescence staining. Scale bars = 30 μm.

Prism 8, San Diego, CA). P value < 0.05 was accepted as significant.

RESULT

Low-Dose Losartan Effectively Alleviated Liver Fibrosis by Interfering RhoA/ROCK Signaling in Mice That Received Partial IVC Ligation

The spleen-to-body and liver-to-body weight ratios were significantly higher in IVCL group than Sham group, suggesting liver congestion and damage in mice that received partial IVC ligation (Fig. 2*A*). Interestingly, the administration of low-dose losartan to mice that received partial IVC ligation kept the spleen-to-body and liver-to-body weight ratios at a comparable level as the mice that received sham operation (Fig. 2*A*). However, the levels of ALT and AST in serum were not significantly different among all groups (Fig. 2*B*).

Masson's trichrome staining showed that the liver tissues from mice that received sham operation revealed normal lobular architecture with few collagen deposition (Fig. 2*C*). The fibrotic area in liver tissues from mice that received partial IVC ligation was obviously increased, and the lobular architecture surrounding fibrotic area was obviously disturbed (Fig. 2*C*). However, these changes in livers following partial IVC ligation were effectively alleviated by low-dose losartan treatment ($P < 0.01$ vs. IVCL group; Fig. 2*C*).

When compared with the Sham group, the proportion of TUNEL-labeled apoptotic cells in liver was significantly increased in IVCL group ($P < 0.05$ vs. Sham group), but was not significantly changed in Losartan group (Fig. 3). The expression of α-SMA, a marker for activated HSCs, was more extensively detected in the liver of IVCL group than that of Sham group. Semiquantitative data also confirmed the enhanced expression of α-SMA in liver of mice from the IVCL group ($P < 0.01$ vs. Sham group; Fig. 3). The enhanced expression of α-SMA in liver induced by partial IVC ligation was significantly decreased by losartan treatment ($P < 0.01$ vs. IVCL group), although there was still significant difference between Losartan group and Sham group (Fig. 3).

We also investigated the expression of several molecules related to RhoA/ROCK signaling because of their central role on mechanotransduction. Although the expression of ROCK2 in liver cells was hardly changed (Fig. 4), RhoA and ROCK1 were obviously upregulated in liver cells surrounding the portal vein from mice that received partial IVC ligation. When compared with the Sham group, semiquantitative data also confirmed that the expression of RhoA and ROCK1 in liver cells was significantly increased in IVCL group ($P < 0.01$ vs. Sham group; Fig. 4). However, the enhanced expression of RhoA and ROCK1 in mice that received partial IVC ligation was effectively attenuated by losartan treatment ($P < 0.01$ vs. Losartan group; Fig. 4). In consistent with the upregulated expression of RhoA and ROCK1, the expression of p-MLC2, a downstream molecule of ROCK, was also significantly upregulated in mice that received partial IVC ligation ($P < 0.01$ vs. Sham group) but was effectively attenuated by losartan treatment ($P < 0.01$ vs. Losartan group; Fig. 4). All these findings from in vivo experiments suggest that low-dose losartan is able to alleviate liver fibrosis by interfering RhoA/ROCK signaling pathway.

Losartan Mitigated the Alteration of Mechanotransduction Properties of HSCs Induced by Ex Vivo Hydrostatic Pressure Loading

To further demonstrate the molecular and cellular mechanisms of losartan on alleviating liver fibrosis, we tried to mimic the elevated intrahepatic hydrostatic pressure in

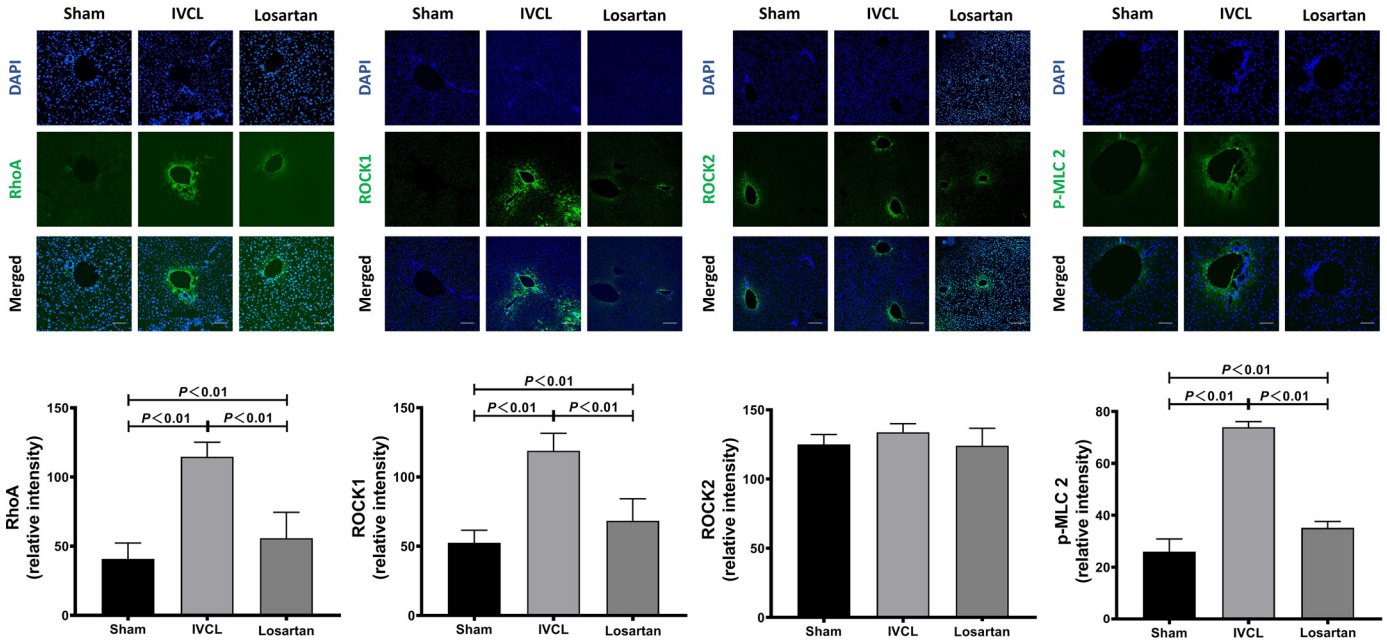

Figure 4. Expression of RhoA, ROCK1, ROCK2, and p-MLC2 in liver of mice after treatment. Representative images (*top*) and semiquantitative data (*bottom*) on the immunofluorescence staining. Scale bars = 30 μm.

partial IVC ligation model by ex vivo approach. Losartan mitigated the upregulation of *AT1R* in HSCs with loading to 50 mmHg for 24 h ($P < 0.01$ vs. 50 mmHg without losartan in medium; Fig. 5*A*). Immunofluorescence staining also showed that the loading of HSCs to 50 mmHg for 24 h significantly enhanced the total expression of AT1R ($P < 0.01$ vs. 0 mmHg) and changed their distribution in cytoplasm and nucleus (Fig. 5, *B* and *C*), but losartan effectively canceled these changes (Fig. 5, *B* and *C*).

Moreover, loading HSCs to 50 mmHg pressure for 24 h significantly upregulated *ACTA2*, *TGFB1*, and *COL1A1* ($P < 0.01$ vs. 0 mmHg; Fig. 6*A*). Immunofluorescence staining also confirmed the enhanced expression of α-SMA, TGF-β_1, and collagen 1 in protein level ($P < 0.01$ vs. 0 mmHg; Fig. 6*B*). As expected, losartan effectively mitigated the hydrostatic pressure loading-induced enhancement on the expression of α-SMA, collagen 1, and TGF-β_1 ($P < 0.01$ vs. 50 mmHg without losartan in medium; Fig. 6, *A* and *B*).

We also found that loading HSCs to 50 mmHg for 24 h significant upregulated the expression of RhoA and ROCK1 in mRNA and protein levels, which were effectively canceled by losartan (Fig. 7, *A* and *B*). However, neither hydrostatic pressure nor losartan treatment significantly changed the expression of ROCK2 in HSCs (Fig. 7, *A* and *B*). Phalloidin staining for F-actin revealed that HSCs loading to 50 mmHg hydrostatic pressure exhibited thick actin bundles and formed a dense parallel network (Fig. 8). Losartan effectively reduced the formation of actin stress fibers in HSCs with 50 mmHg hydrostatic pressure loading (Fig. 8). In addition, 24 h loading to 50 mmHg hydrostatic pressure upregulated the expression of p-MLC2 in HSCs ($P < 0.01$ vs. 0 mmHg; Fig. 8), which was effectively canceled by

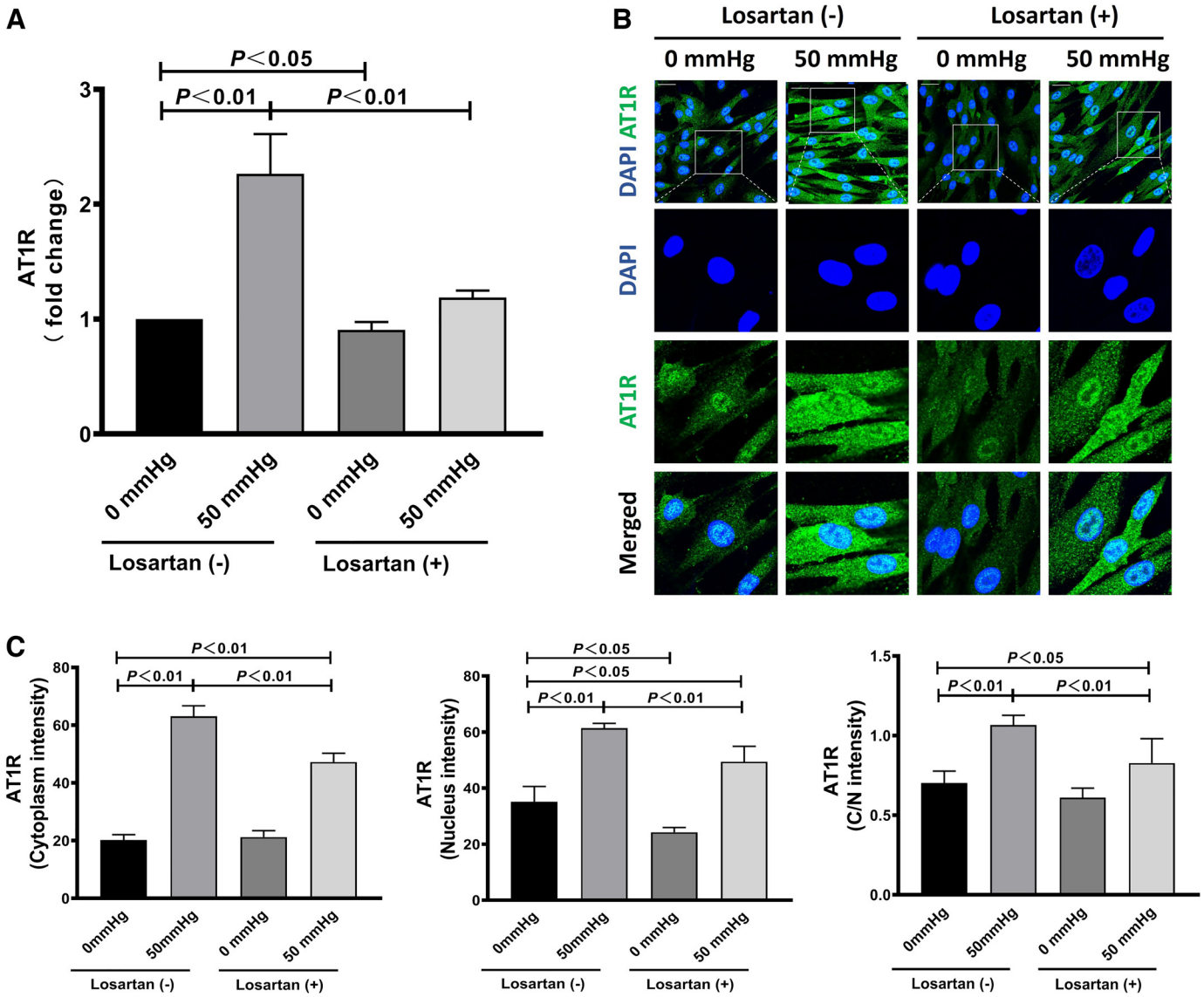

Figure 5. Expression of AT1R in human hepatic stellate cells (HSCs). HSCs were loaded to 50 mmHg for 24 h with or without the addition of losartan in medium. *A*: quantitative RT-PCR data on the fold-change of mRNA expression levels (vs. 0 mmHg). Representative images (*B*) and semiquantitative data (*C*) on the intensity of immunofluorescence staining are shown. Scale bars = 30 μm. Data are represented as means ± SD from three independent experiments.

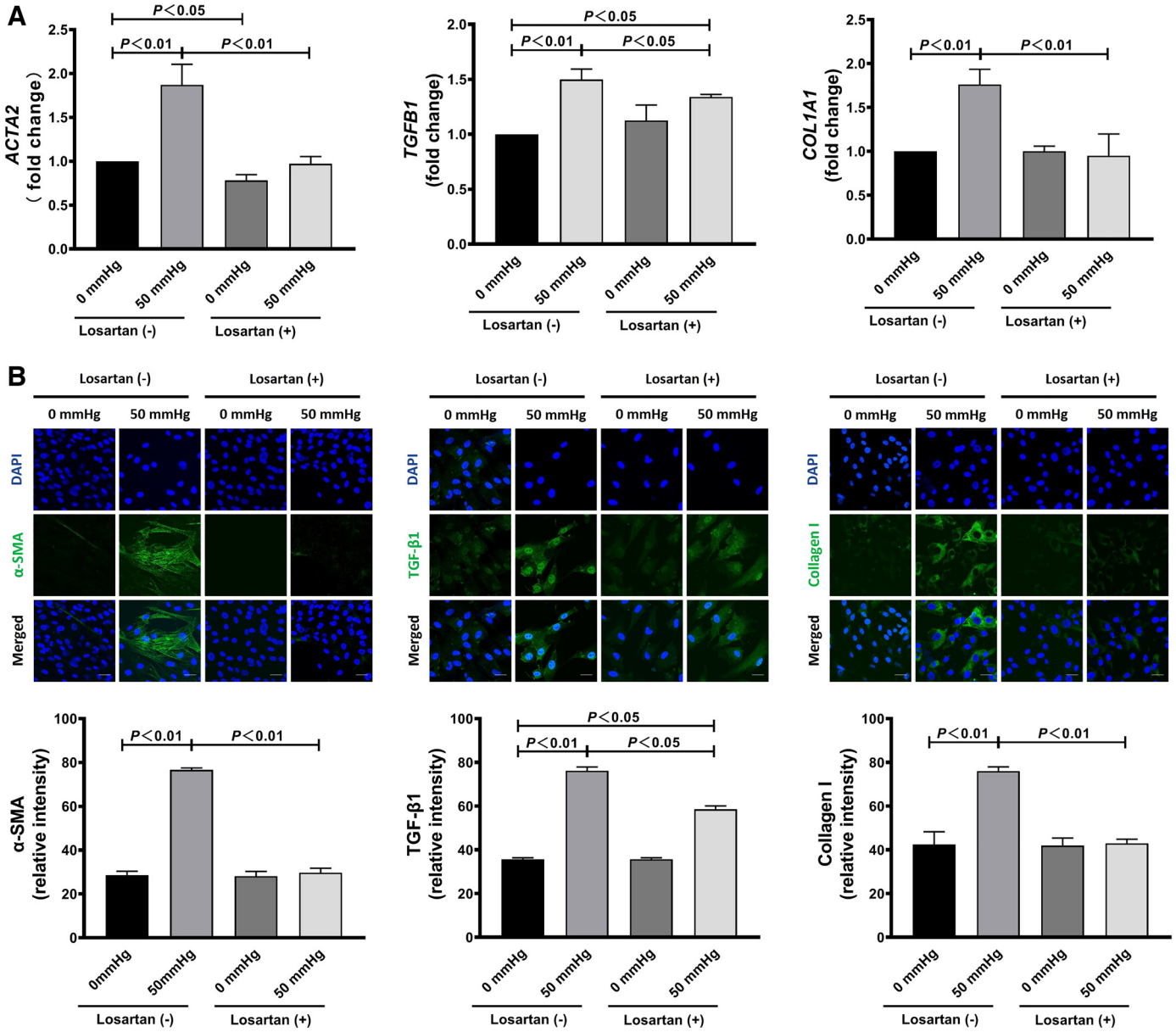

Figure 6. Expression of α-SMA, TGF-β_1, and collagen 1 in human hepatic stellate cells (HSCs). HSCs were loaded to 50 mmHg for 24 h with or without the addition of losartan in medium. *A*: quantitative RT-PCR data on the fold-change of mRNA expression levels (vs. 0 mmHg). *B*: representative images (*top*) and semiquantitative data (*bottom*) on the immunofluorescence staining. Scale bars = 30 μm. Data are represented as means ± SD from three independent experiments.

losartan ($P < 0.01$ vs. 50 mmHg without losartan in medium; Fig. 8). Together, these ex vivo experimental data indicate that losartan can effectively mitigate the hydrostatic pressure-induced alternation of mechanotransduction properties of HSCs.

DISCUSSION

In the present study, we tried to investigate the probable role and relevant mechanism of low-dose ARB in alleviating mechanical stress-induced liver fibrosis. Data from our in vivo and ex vivo studies indicated that losartan effectively alleviated liver fibrosis, likely by modulating the mechanotransduction properties of HSCs.

The dynamic changes of various biomechanics, such as extracellular matrix and interstitial fluid hydrostatic pressure, have been proved to regulate the behaviors and functions of liver cells through mechanosensing and mechanotransduction signalings (12, 13), which thereby contributes to the development and progression of liver diseases. The interstitial fluid hydrostatic pressure is commonly elevated in diseased liver (18, 19). However, it is still poorly understood the role and mechanism of elevated hydrostatic pressure on liver fibrosis because in vivo evaluations are largely limited by the complex biomechanical forces within the microenvironment under different pathological conditions. In this study, we developed a liver fibrosis model by partially ligating the IVC to increase the

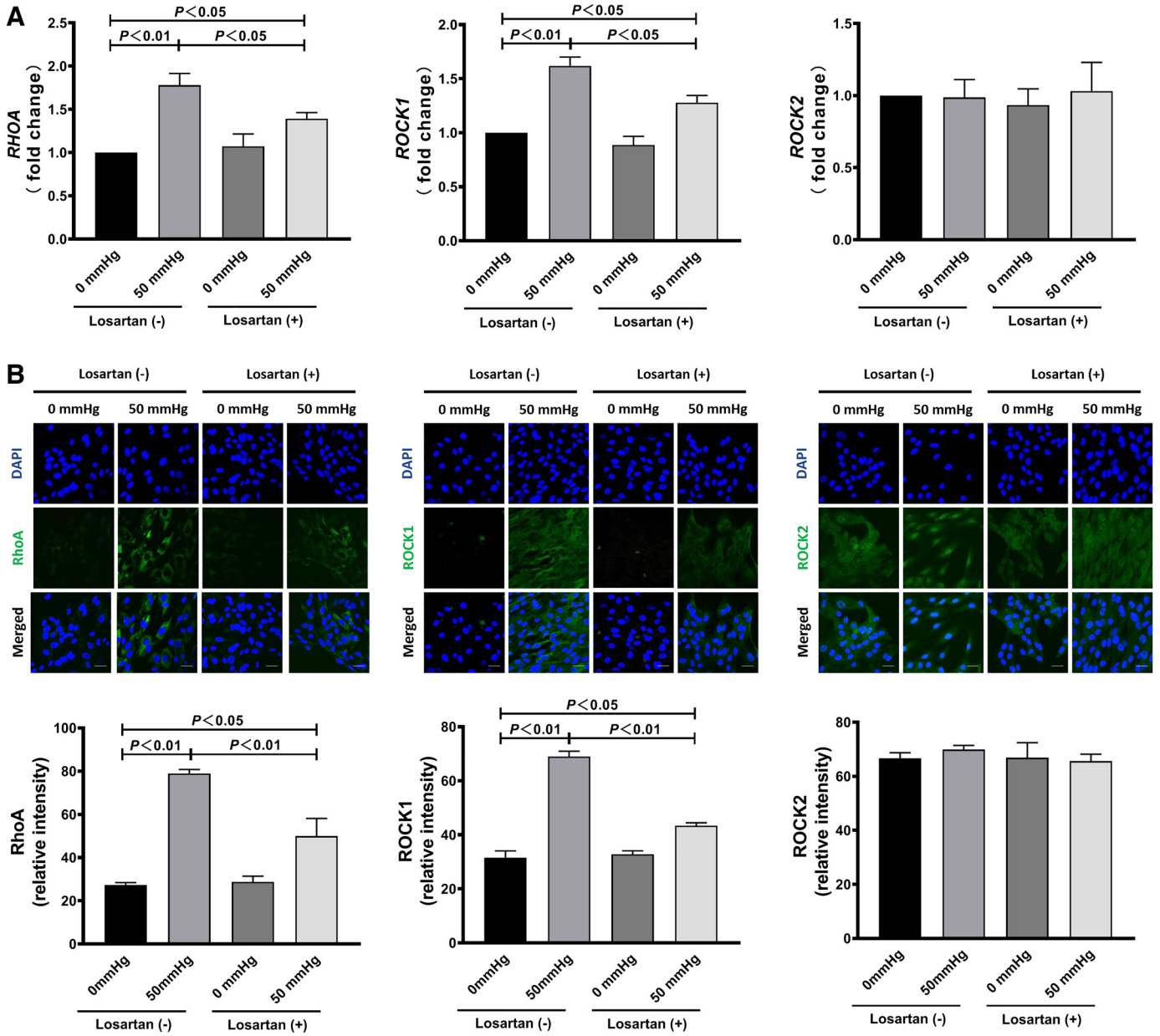

Figure 7. Expression of RhoA, ROCK1, and ROCK2 in human hepatic stellate cells (HSCs). HSCs were loaded to 50 mmHg for 24 h with or without the addition of losartan in medium. *A*: quantitative RT-PCR data on the fold-change of mRNA expression levels (vs. 0 mmHg). *B*: representative images (*top*) and semiquantitative data (*bottom*) on the immunofluorescence staining. Scale bars = 30 μm. Data are represented as means ± SD from three independent experiments.

intrahepatic hydrostatic pressure and used a pneumatic pressurizing system to mimic the elevated intrahepatic hydrostatic pressure ex vivo. The combination of in vivo and ex vivo approaches enables us to investigate the potential effect and relevant molecular/cellular mechanisms of hydrostatic pressure on liver fibrosis.

There is accumulating experimental evidence that ARB may be beneficial to fibrosis in various tissues/organs, including the kidney, heart, and lung by decreasing the production of extracellular matrix proteins from the activated myofibroblasts (20–24). Moreover, previous study has demonstrated that targeting delivery of losartan to HSCs markedly reduces advanced liver fibrosis (25). Losartan has been used over a wide dose range for animal experiments, but the most of studies use around 3–30 mg/kg in rats and mice (26–30). However, a low dosage of losartan (1 mg/kg) has shown significant vasodilation and antihypertensive action in spontaneous or induced hypertensive rats (31, 32). Otherwise, there are a few reports about losartan-induced liver injury (33), although severe hepatotoxicity of losartan rarely happens with a regular dose for the treatment of hypertension. Considering the potential side effect of long-term losartan treatment, including the possibility of directly inducing liver injury, we decided to test a very low-dose losartan (0.5 mg/kg) in this study. The minimized vasodilation effect at a very low dose of losartan will also be useful to clearly detect the

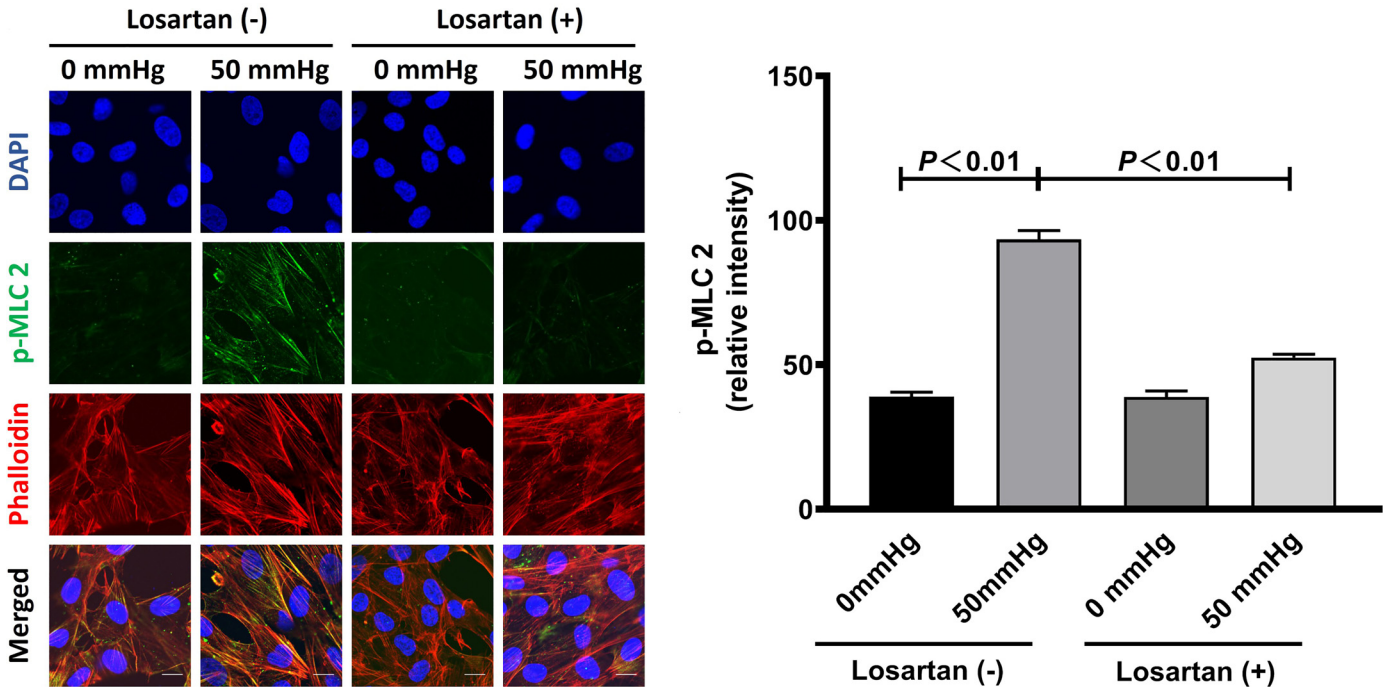

Figure 8. Formation of F-actin and the expression of p-MLC2 in human hepatic stellate cells (HSCs). HSCs were loaded to 50 mmHg for 24 h with or without the addition of losartan in medium. HSCs were triple-stained with p-MLC2 antibody (green), phalloidin (red), and DAPI (blue), and semiquantitative data (*right* bar graph) on the p-MLC2 immunofluorescence intensity of staining. Scale bars = 30 μm. Data are represented as means ± SD from three independent experiments.

potential role of losartan in mechanotransduction regulation. Our data showed that a very low-dose losartan significantly inhibited the activation of HSCs and effectively reduced the fibrotic area in liver of mice that received partial IVC ligation.

About the molecular mechanism, previous studies have already demonstrated that RhoA/ROCK signaling is activated in fibrosis liver (34, 35). As one of the mechanotransduction pathways, RhoA/ROCK signaling is known to regulate the expression of α-SMA and MLC (36, 37). It is also known that RhoA/ROCK pathway activation is regulated by AT1R via promoting actin cytoskeleton polymerization (38). Agreed well with these previous studies, our data indicated that low-dose losartan almost completely attenuated the enhanced expression of RhoA, ROCK1, α-SMA, and p-MLC2 in liver of mice that received partial IVC ligation. Therefore, it seems that losartan relieves partial IVC ligation-induced liver fibrosis by interfering mechanotransduction signaling of HSCs.

To further directly confirm the regulatory role of losartan on mechanotransduction properties of HSCs, we loaded human HSCs to 20 and 50 mmHg hydrostatic pressure using a pneumatic pressurizing system based on previous reports (15, 16). As our preliminary experiment indicated that the loading to 50 mmHg hydrostatic pressure for 24 h clearly induced the shifting of HSCs to profibrotic characteristics without obvious cell damage, we used 50 mmHg hydrostatic pressure for the formal experiments in this study. We used 10 nM losartan for ex vivo experiments because 10 nM is the half-maximal 50% inhibitory concentration of angiotensin II binding to rat hepatocyte nuclei (39) and the concentration of effectively inhibiting angiotensin II-induced rat mesenteric artery contraction (40). This ex vivo experimental approach not only mimics the elevated intrahepatic hydrostatic pressure but also excludes the intrahepatic pressure that fluctuates result of the vasodilator properties of ARB (41).

As a mechanosensitive molecule (11), the ex vivo loading of HSCs to 50 mmHg hydrostatic pressure upregulated AT1R expression and induced their redistribution in cytoplasm and nucleus. Previous study has demonstrated that the activated HSCs synthesize angiotensin II (42). Although we did not measure the level of angiotensin II in medium, the synthesized angiotensin II from activated HSCs may not be enough to change the AT1R expression in HSCs as observed in this study (9). Therefore, we believe losartan may prevent hydrostatic pressure-induced HSC activation at least partly by interfering with the expression of AT1R. Besides, enhanced F-actin formation and increased expressions of RhoA/ROCK and MLC2 were observed in HSCs. These molecules determine the organization and plasticity of cytoskeleton (43) and are well known as the second messenger of cellular mechanotransduction (36). Moreover, the expressions of α-SMA, TGF-β, and several profibrotic molecules were also upregulated in HSCs in response to 50 mmHg hydrostatic pressure loading. However, losartan effectively attenuated the alternation of mechanotransduction properties in HSCs caused by hydrostatic pressure loading.

In conclusion, data from our ex vivo and in vivo experiments clearly indicated that a very low dose of losartan effectively alleviated liver fibrosis, likely by modulating the mechanotransduction properties of HSCs. Uncovering the biomechanical signaling pathway of ARB treatment on

liver fibrosis will be helpful to develop novel molecular targeting therapy for liver diseases.

SUPPLEMENTAL DATA

Supplemental Tables S1–S3: https://doi.org/10.6084/m9.figshare.18133628.

ACKNOWLEDGMENTS

The graphical abstract presented in this study was created with BioRender.com with permission.

GRANTS

This work was supported by a Grant-in-Aid for the Ministry of Education, Science, Sports, Culture and Technology of Japan and collaborative Research program of the Atomic-bomb Disease Institute of Nagasaki University. The funder played no role in the study design, data collection and analysis, decision to publish, or preparation of the manuscript.

DISCLOSURES

No conflicts of interest, financial or otherwise, are declared by the authors.

AUTHOR CONTRIBUTIONS

W.G. and T.-S.L conceived and designed research; Z.H., P.L. and M.O.K. performed experiments; Z.H. and Y. H. analyzed data; Z.H. prepared figures; W.G. and T.-S.L. edited and revised manuscript; W.G. and T.-S.L. approved final version of manuscript.

REFERENCES

1. **Wells RG.** Tissue mechanics and fibrosis. *Biochim Biophys Acta* 1832: 884–890, 2013. doi:10.1016/j.bbadis.2013.02.007.
2. **Wynn TA.** Cellular and molecular mechanisms of fibrosis. *J Pathol* 214: 199–210, 2008. doi:10.1002/path.2277.
3. **Seki E**, **Schwabe RF.** Hepatic inflammation and fibrosis: functional links and key pathways. *Hepatology* 61: 1066–1079, 2015. doi:10.1002/hep.27332.
4. **Huang C**, **Liu L**, **You Z**, **Zhao Y**, **Dong J**, **Du Y**, **Ogawa R.** Endothelial dysfunction and mechanobiology in pathological cutaneous scarring: lessons learned from soft tissue fibrosis. *Br J Dermatol* 177: 1248–1255, 2017. doi:10.1111/bjd.15576.
5. **Carver W**, **Goldsmith EC.** Regulation of tissue fibrosis by the biomechanical environment. *Biomed Res Int* 2013: 101979, 2013. doi:10.1155/2013/101979.
6. **Nagy JA**, **Benjamin L**, **Zeng H**, **Dvorak AM**, **Dvorak HF.** Vascular permeability, vascular hyperpermeability and angiogenesis. *Angiogenesis* 11: 109–119, 2008. doi:10.1007/s10456-008-9099-z.
7. **Olsen AL**, **Bloomer SA**, **Chan EP**, **Gaça MDA**, **Georges PC**, **Sackey B**, **Uemura M**, **Janmey PA**, **Wells RG.** Hepatic stellate cells require a stiff environment for myofibroblastic differentiation. *Am J Physiol Gastrointest Liver Physiol* 301: G110–G118, 2011. doi:10.1152/ajpgi.00412.2010.
8. **Zhubanchaliyev A**, **Temirbekuly A**, **Kongrtay K**, **Wanshura LC**, **Kunz J.** Targeting mechanotransduction at the transcriptional level: YAP and BRD4 are novel therapeutic targets for the reversal of liver fibrosis. *Front Pharmacol* 7: 462, 2016. doi:10.3389/fphar.2016.00462.
9. **Zou Y**, **Akazawa H**, **Qin Y**, **Sano M**, **Takano H**, **Minamino T**, **Makita N**, **Iwanaga K**, **Zhu W**, **Kudoh S**, **Toko H**, **Tamura K**, **Kihara M**, **Nagai T**, **Fukamizu A**, **Umemura S**, **Iiri T**, **Fujita T**, **Komuro I.** Mechanical stress activates angiotensin II type 1 receptor without the involvement of angiotensin II. *Nat Cell Biol* 6: 499–506, 2004. doi:10.1038/ncb1137.
10. **Mederos y Schnitzler M**, **Storch U**, **Meibers S**, **Nurwakagari P**, **Breit A**, **Essin K**, **Gollasch M**, **Gudermann T.** Gq-coupled receptors as mechanosensors mediating myogenic vasoconstriction. *EMBO J* 27: 3092–3103, 2008. doi:10.1038/emboj.2008.233.
11. **Mederos y Schnitzler M**, **Storch U**, **Gudermann T.** AT1 receptors as mechanosensors. *Curr Opin Pharmacol* 11: 112–116, 2011. doi:10.1016/j.coph.2010.11.003.
12. **Ma Z-G**, **Yuan Y-P**, **Wu H-M**, **Zhang X**, **Tang Q-Z.** Cardiac fibrosis: new insights into the pathogenesis. *Int J Biol Sci* 14: 1645–1657, 2018. doi:10.7150/ijbs.28103.
13. **Yamakawa T**, **Tanaka S**, **Numaguchi K**, **Yamakawa Y**, **Motley ED**, **Ichihara S**, **Inagami T.** Involvement of Rho-kinase in angiotensin II-induced hypertrophy of rat vascular smooth muscle cells. *Hypertension* 35: 313–318, 2000. doi:10.1161/01.hyp.35.1.313.
14. **Yao S**, **Feng D**, **Wu Q**, **Li K**, **Wang L.** Losartan attenuates ventilator-induced lung injury. *J Surg Res* 145: 25–32, 2008. doi:10.1016/j.jss.2007.03.075.
15. **Sawada Y**, **Kawaratani H**, **Kubo T**, **Fujinaga Y**, **Furukawa M**, **Saikawa S**, **Sato S**, **Seki K**, **Takaya H**, **Okura Y**, **Kaji K**, **Shimozato N**, **Mashitani T**, **Kitade M**, **Moriya K**, **Namisaki T**, **Akahane T**, **Mitoro A**, **Yamao J**, **Yoshiji H.** Combining probiotics and an angiotensin-II type 1 receptor blocker has beneficial effects on hepatic fibrogenesis in a rat model of non-alcoholic steatohepatitis. *Hepatol Res* 49: 284–295, 2019. doi:10.1111/hepr.13281.
16. **Simonetto DA**, **Yang H**, **Yin M**, **de Assuncao TM**, **Kwon JH**, **Hilscher M**, **Pan S**, **Yang L**, **Bi Y**, **Beyder A**, **Cao S**, **Simari RD**, **Ehman R**, **Kamath PS**, **Shah VH.** Chronic passive venous congestion drives hepatic fibrogenesis via sinusoidal thrombosis and mechanical forces. *Hepatology* 61: 648–659, 2015. doi:10.1002/hep.27387.
17. **Yoshino D**, **Funamoto K**, **Sato K**, **Kenry** , **Sato M**, **Lim CT.** Hydrostatic pressure promotes endothelial tube formation through aquaporin 1 and Ras-ERK signaling. *Commun Biol* 3: 152, 2020. doi:10.1038/s42003-020-0881-9.
18. **Okada Y**, **Tsuzuki Y**, **Hokari R**, **Miyazaki J**, **Matsuzaki K**, **Mataki N**, **Komoto S**, **Watanabe C**, **Kawaguchi A**, **Nagao S**, **Itoh K**, **Miura S.** Pressure loading and ethanol exposure differentially modulate rat hepatic stellate cell activation. *J Cell Physiol* 215: 472–480, 2008. doi:10.1002/jcp.21329.
19. **Chen G**, **Xia B**, **Fu Q**, **Huang X**, **Wang F**, **Chen Z**, **Lv Y.** Matrix mechanics as regulatory factors and therapeutic targets in hepatic fibrosis. *Int J Biol Sci* 15: 2509–2521, 2019. doi:10.7150/ijbs.37500.
20. **Grace JA**, **Herath CB**, **Mak KY**, **Burrell LM**, **Angus PW.** Update on new aspects of the renin–angiotensin system in liver disease: clinical implications and new therapeutic options. *Clin Sci (Lond)* 123: 225–239, 2012. doi:10.1042/CS20120030.
21. **Couluris M**, **Kinder BW**, **Xu P**, **Gross-King M**, **Krischer J**, **Panos RJ.** Treatment of idiopathic pulmonary fibrosis with losartan: a pilot project. *Lung* 190: 523–527, 2012. doi:10.1007/s00408-012-9410-z.
22. **Lim DS**, **Lutucuta S**, **Bachireddy P**, **Youker K**, **Evans A**, **Entman M**, **Roberts R**, **Marian AJ.** Angiotensin II blockade reverses myocardial fibrosis in a transgenic mouse model of human hypertrophic cardiomyopathy. *Circulation* 103: 789–791, 2001. doi:10.1161/01.cir.103.6.789.
23. **Tzanidis A**, **Lim S**, **Hannan RD**, **See F**, **Ugoni AM**, **Krum H.** Combined angiotensin and endothelin receptor blockade attenuates adverse cardiac remodeling post-myocardial infarction in the rat: possible role of transforming growth factor β(1). *J Mol Cell Cardiol* 33: 969–981, 2001. doi:10.1006/jmcc.2001.1361.
24. **Boffa J-J**, **Lu Y**, **Placier S**, **Stefanski A**, **Dussaule J-C**, **Chatziantoniou C.** Regression of renal vascular and glomerular fibrosis: role of angiotensin II receptor antagonism and matrix metalloproteinases. *J Am Soc Nephrol* 14: 1132–1144, 2003. doi:10.1097/01.asn.0000060574.38107.3b.
25. **Moreno M**, **Gonzalo T**, **Kok RJ**, **Sancho-Bru P**, **van Beuge M**, **Swart J**, **Prakash J**, **Temming K**, **Fondevila C**, **Beljaars L**, **Lacombe M**, **van der Hoeven P**, **Arroyo V**, **Poelstra K**, **Brenner DA**, **Ginès P**, **Bataller R.** Reduction of advanced liver fibrosis by short-term targeted delivery of an angiotensin receptor blocker to hepatic stellate cells in rats. *Hepatology* 51: 942–952, 2010. doi:10.1002/hep.23419.
26. **Yun HH**, **Park S**, **Chung MJ**, **Son JY**, **Park JM**, **Jung SJ**, **Yim JH**, **Kang KK**, **Byeon S**, **Baek SM**, **Lee SW**, **Lee AR**, **Kim TH**, **Park JK**, **Jeong KS.** Effects of losartan and l-serine in a mouse liver fibrosis model. *Life Sci* 278: 119578, 2021. doi:10.1016/j.lfs.2021.119578.
27. **Wang CH**, **Liu HM**, **Chang ZY**, **Huang TH**, **Lee TY.** Losartan prevents hepatic steatosis and macrophage polarization by inhibiting HIF-1α

in a murine model of NAFLD. *Int J Mol Sci* 22: 7841, 2021. doi:10.3390/ijms22157841.

28. **Wei YH**, **Jun L**, **Qiang CJ.** Effect of losartan, an angiotensin II antagonist, on hepatic fibrosis induced by CCl4 in rats. *Dig Dis Sci* 49: 1589–1594, 2004. doi:10.1023/b:ddas.0000043369.88701.5b.
29. **Czechowska G**, **Celinski K**, **Korolczuk A**, **Wojcicka G**, **Dudka J**, **Bojarska A**, **Madro A**, **Brzozowski T.** The effect of the angiotensin II receptor, type 1 receptor antagonists, losartan and telmisartan, on thioacetamide-induced liver fibrosis in rats. *J Physiol Pharmacol an Off J Polish Physiol Soc* 67: 575–586, 2016.
30. **Wong PC**, **Barnes TB**, **Chiu AT**, **Christ DD**, **Duncia JV**, **Herblin WF**, **Timmermans P.** Losartan (DuP 753), an orally active nonpeptide angiotensin II receptor antagonist. *Cardiovasc Drug Rev* 9: 317–339, 1991. doi:10.1111/j.1527-3466.1991.tb00419.x.
31. **Inada Y**, **Ojima M**, **Kanagawa R**, **Misumi Y**, **Nishikawa K**, **Naka T.** Pharmacologic properties of candesartan cilexetil–possible mechanisms of long-acting antihypertensive action. *J Hum Hypertens* 13, Suppl 1: S75–S80, 1999. doi:10.1038/sj.jhh.1000749.
32. **Navarro-Cid J**, **Maeso R**, **Perez-Vizcaino F**, **Cachofeiro V**, **Ruilope LM**, **Tamargo J**, **Lahera V.** Effects of losartan on blood pressure, metabolic alterations, and vascular reactivity in the fructose-induced hypertensive rat. *Hypertens* 26: 1074–1078, 1995. doi:10.1161/01.hyp.26.6.1074.
33. **Tabak F**, **Mert A**, **Ozaras R**, **Biyikli M**, **Ozturk R**, **Ozbay G**, **Senturk H**, **Aktuglu Y.** Losartan-induced hepatic injury. *J Clin Gastroenterol* 34: 585–586, 2002. doi:10.1097/00004836-200205000-00022.
34. **Klein S**, **Frohn F**, **Magdaleno F**, **Reker-Smit C**, **Schierwagen R**, **Schierwagen I**, **Uschner FE**, **van Dijk F**, **Fürst DO**, **Djudjaj S**, **Boor P**, **Poelstra K**, **Beljaars L**, **Trebicka J.** Rho-kinase inhibitor coupled to peptide-modified albumin carrier reduces portal pressure and increases renal perfusion in cirrhotic rats. *Sci Rep* 9: 2256, 2019. doi:10.1038/s41598-019-38678-5.
35. **Kato M**, **Iwamoto H**, **Higashi N**, **Sugimoto R**, **Uchimura K**, **Tada S**, **Sakai H**, **Nakamuta M**, **Nawata H.** Role of Rho small GTP binding protein in the regulation of actin cytoskeleton in hepatic stellate cells. *J Hepatol* 31: 91–99, 1999. doi:10.1016/S0168-8278(99)80168-8.
36. **Martino F**, **Perestrelo AR**, **Vinarsky V**, **Pagliari S**, **Forte G.** Cellular mechanotransduction: from tension to function. *Front Physiol* 9: 824, 2018. doi:10.3389/fphys.2018.00824.
37. **Burridge K**, **Monaghan-Benson E**, **Graham DM.** Mechanotransduction: from the cell surface to the nucleus via RhoA. *Philos Trans R Soc Lond B Biol Sci* 374: 20180229, 2019. doi:10.1098/rstb.2018.0229.
38. **Qi Y**, **Liang X**, **Dai F**, **Guan H**, **Sun J**, **Yao W.** RhoA/ROCK pathway activation is regulated by AT1 receptor and participates in smooth muscle migration and dedifferentiation via promoting actin cytoskeleton polymerization. *Int J Mol Sci* 21: 5398, 2020. doi:10.3390/ijms21155398.
39. **Booz GW**, **Conrad KM**, **Hess AL**, **Singer HA**, **Baker KM.** Angiotensin-II-binding sites on hepatocyte nuclei. *Endocrinology* 130: 3641–3649, 1992. doi:10.1210/endo.130.6.1597161.
40. **Balt JC**, **Mathy M-J**, **Nap A**, **Pfaffendorf M**, **van Zwieten PA.** Effect of the AT1-receptor antagonists losartan, irbesartan, and telmisartan on angiotensin II-induced facilitation of sympathetic neurotransmission in the rat mesenteric artery. *J Cardiovasc Pharmacol* 38: 141–148, 2001. doi:10.1097/00005344-200107000-00015.
41. **Burnier M.** Angiotensin II type 1 receptor blockers. *Circulation* 103: 904–912, 2001. doi:10.1161/01.cir.103.6.904.
42. **Bataller R**, **Sancho-Bru P**, **Ginès P**, **Lora JM**, **Al-Garawi A**, **Solé M**, **Colmenero J**, **Nicolás JM**, **Jiménez W**, **Weich N**, **Gutiérrez-Ramos J-C**, **Arroyo V**, **Rodés J.** Activated human hepatic stellate cells express the renin-angiotensin system and synthesize angiotensin II. *Gastroenterology* 125: 117–125, 2003. doi:10.1016/s0016-5085(03)00695-4.
43. **Cai S**, **Pestic-Dragovich L**, **O'Donnell ME**, **Wang N**, **Ingber D**, **Elson E**, **De Lanerolle P.** Regulation of cytoskeletal mechanics and cell growth by myosin light chain phosphorylation. *Am J Physiol Cell Physiol* 275: C1349–C1356, 1998. doi:10.1152/ajpcell.1998.275.5.C1349.